Journal of Inorganic and General Chemistry
ZAAC
Zeitschrift für anorganische und allgemeine Chemie
www.zaac.wiley-vch.de
RESEARCH ARTICLE

DOI: 10.1002/zaac.202200207

Magnesium Complexes with Isomeric Pyrazol-4-ylidene and Imidazol-2-ylidene Ligands

Stuart Burnett,[a] Matthew de Vere-Tucker,[a] Matthew Davitt,[a] David B. Cordes,[a] Alexandra M. Z. Slawin,[a] Rochelle Ferns,[a] Tanja van Mourik,[a] and Andreas Stasch*[a]

Dedicated to Professor Cameron Jones on the occasion of his 60th birthday.

Dimagnesium(I) complexes [{(^{Ar}nacnac)Mg}$_2$], where ^{Ar}nacnac = HC(MeCNAr)$_2$, Ar = Dip = 2,6-*i*Pr$_2$–C$_6$H$_3$, Ar = Dep = 2,6-Et$_2$–C$_6$H$_3$, Ar = Mes = 2,4,6-Me$_3$–C$_6$H$_2$, react with iodoarenes in oxidative addition reactions. With iodobenzene, magnesium phenyl and magnesium iodide complex fragments were obtained, and from a reaction with 4-iodo-1,2,3,5-tetramethylpyrazolium iodide, [^{Me}PZI]I, the pyrazol-4-ylidene complex [(^{Dip}nacnac)MgI(^{Me}PZ)] was structurally characterised, alongside other products. The isomeric imidazol-2-ylidene complex [(^{Dip}nacnac)MgI(^{Me}NHC)], where ^{Me}NHC is 1,3,4,5-tetramethylimidazol-2-ylidene, was prepared and characterised. X-ray crystal structure determinations and DFT computational studies have been carried out to compare the related complexes. The results show that the ^{Me}PZ ligand is higher in energy and more nucleophilic than its more common isomeric ^{Me}NHC carbene.

Introduction

N-heterocyclic carbenes including related neutral carbon-based donor molecules such as abnormal, remote and mesoionic carbenes, have found wide-ranging applications in chemistry and are highly valued as strong σ-donor ligands for metal complexes.[1–3] The class of imidazol-2-ylidenes, **A** (Figure 1), is the most commonly used type, but a range of remote or mesoionic carbenes have shown advantageous properties, such as stronger σ-donor abilities, albeit often at the expense of a significantly lower stability of the free carbene species in comparison to **A**.[1,2,4] Dyker, Bertrand and co-workers introduced the cyclic bent allenes **B** and **C** as carbene species,[5,6] see Figure 1. These compounds have been called (cyclic) bent allenes, (remote) carbenes, mesoionic carbenes, carbodicarbenes, carbenoids, zwitterions, and possibly other interpretations, which highlights the different viewpoints that the unusual bonding aspects, structure, and properties in these species can be described as.[7,8] Related to this, Huynh and co-workers reported pyrazol-4-ylidene (pyrazolin-4-ylidene) complexes of palladium, e.g., **D**, which were prepared by oxidative addition of iodopyrazolium salts to palladium(0) complexes.[9,10] These species contain aliphatic or aromatic substituents on the carbon centres adjacent to the central nucleophilic carbon donor.

Results and Discussion

Synthesis and molecular structures

We set out to explore if small pyrazol-4-ylidenes can be stabilised by electropositive main group metals. Dimagnesium(I) complexes[11] seemed to be good candidates for their generation. These highly reducing complexes of general formula LMgMgL, where L is a sterically demanding, typically chelating anionic *N*-ligand such as a β-diketiminate, have demonstrated the ability to reduce a range of challenging carbon-based substrates including, for example, the reversible reduction of selected alkenes,[12] and conversion of C$_{60}$ to its hexaanion.[13] They have also acted as soluble, stoichiometric and strong reducing agents to a range of main group and transition metal halide and hydride complexes to yield new low oxidation state species.[11b] Their ability to activate a range of C–F bonds[14] to afford (nucleophilic) organomagnesium complexes show their suitability for challenging organic halides, RX, where X = halogen. Similarly, rare magnesium(0) complexes react with RX species such as *n*BuI, PhI and PhF to furnish organomagnesium complexes in (homogeneous) molecular reactions to Grignard-like species.[15] Thus, it should be straightforward activating RX species of heavier halides with magnesium(I) complexes and this has been our past experience with this compound class, e.g., the unsuitability of using chlorinated solvents with these compounds due to rapid C–Cl reduction. In comparison, related dizinc(I) compounds also react with RX species and, for example, show slow reaction at room temperature with EtI and EtBr in aromatic solvents, but not with PhI.[16] Outside of molecular low oxidation state complex chemistry, the mecha-

[a] S. Burnett, M. de Vere-Tucker, M. Davitt, Dr. D. B. Cordes, Prof. Dr. A. M. Z. Slawin, R. Ferns, Dr. T. van Mourik, Dr. A. Stasch
EaStCHEM School of Chemistry, University of St Andrews, North Haugh, KY16 9ST St Andrews, United Kingdom
E-mail: as411@st-andrews.ac.uk

Supporting information for this article is available on the WWW under https://doi.org/10.1002/zaac.202200207

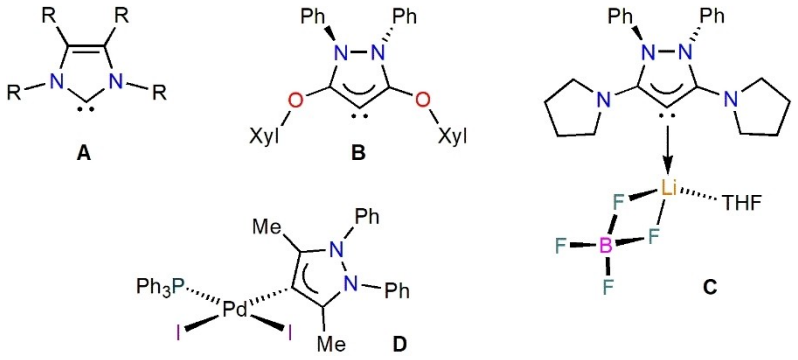

Figure 1. Relevant heterocyclic carbene species; Xyl = 2,6-dimethylphenyl.

nisms of heterogeneous Grignard reagent formation from magnesium metal have been widely studied and are complicated by the heterogenous nature of the system relying on a surface reaction on magnesium metal.[17]

In preliminary reactions with iodoarenes, we have treated [{(^{Ar}nacnac)Mg}$_2$] **1**, where ^{Ar}nacnac = HC(MeCNAr)$_2$, Ar = Dip = 2,6-*i*Pr$_2$–C$_6$H$_3$ **1a**,[18] Ar = Dep = 2,6-Et$_2$–C$_6$H$_3$ **1b**,[19] Ar = Mes = 2,4,6-Me$_3$–C$_6$H$_2$ **1c**,[20] with iodobenzene in deuterated benzene at room temperature. These reactions proceeded rapidly and cleanly in aromatic solvents for Ar = Dip and Mes, and slightly slower for Ar = Dep, to yield either [(^{Dip}nacnac)MgPh] **2a**[21] and poorly soluble [{(^{Dip}nacnac)MgI}$_2$] **3a**[22] for Ar = Dip, or the asymmetrically bridged complexes [{(^{Ar}nacnac)Mg}$_2$(μ-Ph)(μ-I)] for Ar = Dep (**4b**) or Mes (**4c**), respectively, as judged by NMR spectroscopy, see Scheme 1. The slightly different outcomes in these reactions are due to steric effects with [(^{Dip}nacnac)MgPh] **2a** showing a monomeric structure,[21] whereas **4b** and **4c** form stable asymmetric bridging species according to NMR spectroscopic studies. The asymmetrically bridged species **4b**,**c** are furthermore thermally stable and the ligands do not rapidly redistribute easily, i.e., the Schlenk-equilibrium appears to be supressed. For example, they show no significant decomposition or redistribution after 16 hours at 100 °C in deuterated benzene. However, small quantities of the respective iodide complexes [{(^{Ar}nacnac)MgI}$_2$] **3b**,**c** can be formed alongside **4b**,**c**. For example, storing **4c** for a prolonged time in solution or as part of mixtures will eventually form some [{(^{Mes}nacnac)MgI}$_2$] **3c**[20] that is driven by crystallisation. So far, we have not been able to structurally characterise **4b** or **4c**, or crystallise analytically pure crops. NMR spectroscopy revealed the asymmetry of the resonances for the aryl groups in **4b**,**c** above and below the β-diketiminate magnesium plane, and the resonances for the bridging phenyl group are similar to those found in the related complex [{(^{Mes}nacnac)Mg}$_2$(μ-Ph)(μ-H)].[23] A range of different coordination modes of bridging phenyl groups was very recently revealed for related β-diketiminate calcium complexes.[24] These reactions again show the higher reactivity of dimagnesium(I) compounds, here towards PhI, compared with those of dizinc(I) complexes.[16]

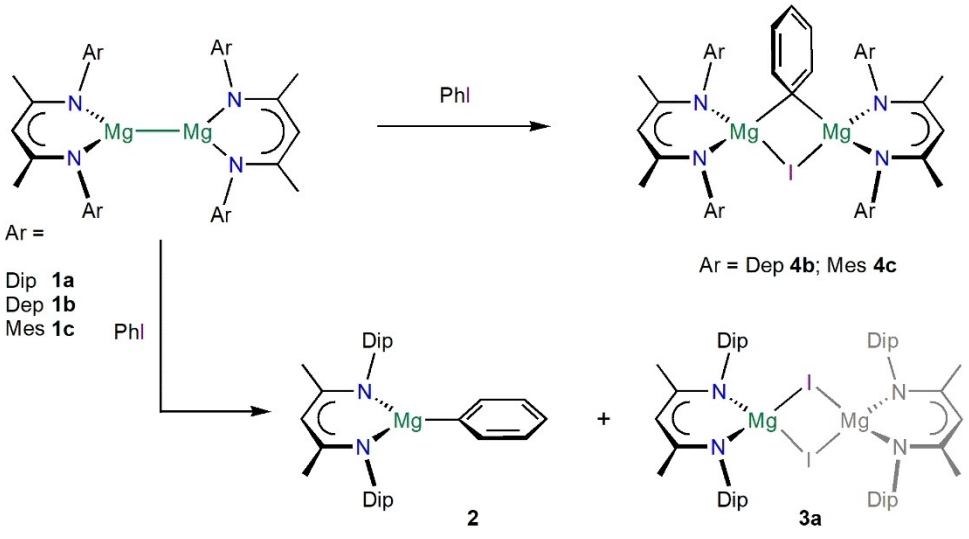

Scheme 1. Reaction of [{(^{Ar}nacnac)Mg}$_2$] **1** with PhI.

As suitable starting materials towards pyrazol-4-ylidene complexes, we prepared two small 1,2,3,5-tetraalkyl-4-iodopyrazolium iodide salts from the respective 4-iodopyrazole and iodomethane, as described previously.[9,10,25] The reactions of these salts [^{Me}PZI]I **5a** (4-iodo-1,2,3,5-tetramethylpyrazolium iodide) and [^{Et}PZI]I **5b** (3,5-diethyl-4-iodo-1,2-dimethylpyrazolium iodide), see Scheme 2, with one equivalent of dimagnesium(I) complexes [{(^{Ar}nacnac)Mg}$_2$] **1a,b** in toluene, benzene or hexane proceeded slowly at room temperature. The reaction mixtures are suspensions, due to the poor solubility of the salts, that slowly lose the yellow colour of the magnesium complexes and form product mixtures dominated by [{(^{Ar}nacnac)MgI}$_2$] **3a,b** and other magnesium iodide species, see Scheme 2. Similar product mixtures were obtained when the reactions were carried out at elevated temperatures. The cationic nature of the iodopyrazolium salts **5a,b** should allow for a fast reduction with dimagnesium(I) complexes, as with iodobenzene, but the poor solubility of the salts render these reactions relatively slow in practice. NMR spectroscopic studies from *in-situ* reactions typically showed ^{1}H NMR resonances of four to five main species that contain β-diketiminate ligands in the reaction mixtures. Similarly, the precipitates from these reactions also showed to be product mixtures of several complexes including large quantities of poorly soluble [{(^{Ar}nacnac)MgI}$_2$] **3a,b**. ^{13}C{^{1}H} NMR spectra of these mixtures could not be assigned and provided no observed unusual ^{13}C NMR resonance. Separation attempts by fractionalised crystallisation failed to yield pure crops of compounds so far and increasingly afforded further formation and precipitation of [{(^{Ar}nacnac)MgI}$_2$] **3a,b** over time. However, from these reactions, several complexes could be structurally characterised, including the target complex [(^{Dip}nacnac)MgI(^{Me}PZ)] **6a**, see Figure 2, and the by-product salts [^{Me}PZI][(^{Dep}nacnac)MgI$_2$] **7ab** and [^{Et}PZI][(^{Dip}nacnac)MgI$_2$] **7ba**, see Figures 3 and 4. Other attempts of reductions of [^{Me}PZI]I **5a** using reducing agents such as potassium metal afforded product mixtures including poorly soluble compounds.

The molecular structure of [(^{Dip}nacnac)MgI(^{Me}PZ)] **6a** contains a β-diketiminate-chelated, distorted tetrahedral Mg centre with an Mg–I bond of 2.7420(10) Å and an Mg–C bond of 2.168(3) Å to the neutral pyrazol-4-ylidene ligand. The C–C bond lengths in the ^{Me}PZ ligand are broadly similar to those in **B** and **C**, but the C30–C31–C32 bond angle (103.3(2)°) is slightly wider than related ones in **B** (97.5(2)°) and **C** (100.8(1)°). The structural features of **6a** will be discussed and compared in more detail below.

Complexes [^{Me}PZI][(^{Dep}nacnac)MgI$_2$] **7ab** and [^{Et}PZI][(^{Dip}nacnac)MgI$_2$] **7ba** are diiodido-β-diketiminate magnesate complexes with 4-iodo-pyrazolium cations. Selected metrical data is collected in the Figure captions and in Table 1 for

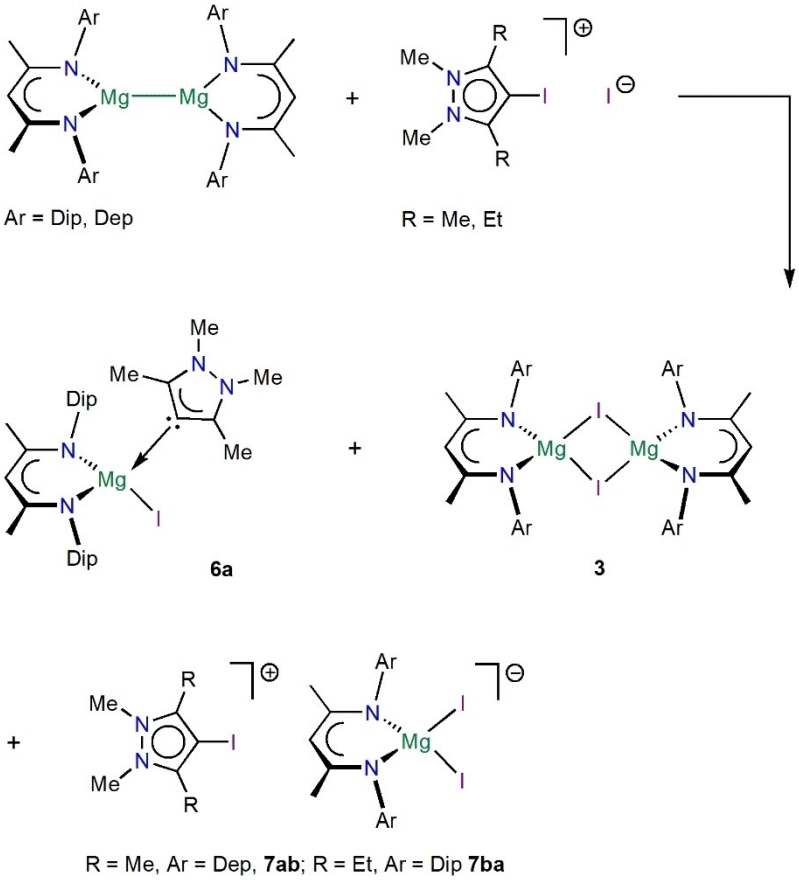

Scheme 2. Reactions of **1** with iodopyrazolium salts **5**.

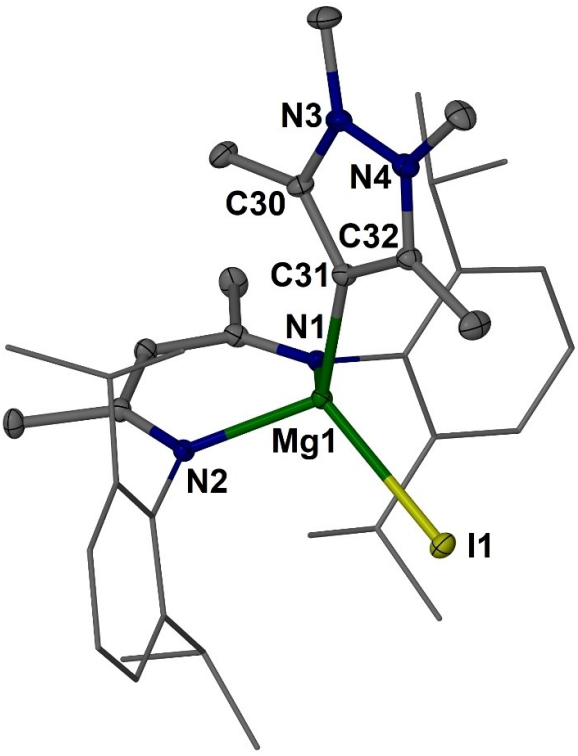

Figure 2. Molecular structure (30 % thermal ellipsoid) of complex **6a**·C_6H_6. Hydrogen atoms and solvent molecule omitted for clarity. Dip groups are shown as wireframe. Selected angles (°): N2–Mg1–N1 92.06(10), C31–Mg1–I1 111.50(8), C30–C31–C32 103.3(2). Selected distances for the molecule are collected in Figure 8.

the cation. For comparison we have also prepared and structurally characterised the 2-iodo-imidazolium iodide salt [^{Me}NHCI]I **8** (2-iodo-1,3,4,5-tetramethylimidazolium iodide) from ^{Me}NHC and iodine in THF, see Figure 5, and selected bond distances are collected in Table 1. As part of this study [^{Me}PZH]I was also structurally characterised and is presented in the supporting information. The bond distances within the rings of **7ab**, **7ba** and **8** are not largely different from those in the respective carbene species, vide infra.

For more detailed comparison to **6a** we have prepared the imidazol-2-ylidene magnesium complexes [(^{Dip}nacnac)MgI(^{Me}NHC)] **9a** and [(^{Dip}nacnac)MgI(^{Et}NHC)] **9b**, with ^{Et}NHC = 1,3-diethyl-4,5-dimethylimidazol-2-ylidene, from [(^{Dip}nacnac)MgI(OEt_2)] with the respective free *N*-heterocyclic carbene in toluene, see Scheme 3, and Figures 6 and 7. NHC ligands are commonly employed in organometallic main group chemistry and a range of examples are known for magnesium.[3] For example, monomeric complexes with *N,N'*-chelating ligands and a halide[26] or reactive anionic ligands[27] have been prepared. NHCs can even coordinate to, and be activated by, magnesium(I) complexes,[28] and a related reduced magnesium complex with a cyclic (alkyl)(amino)carbene radical anion has been characterised.[29] Both complexes **9a** and **9b** show the expected structures with distorted tetrahedrally coordinated Mg centres. Metrical data for complex **9a**, which is a constitutional (structural) isomer of **6a**, is presented in more detail in the next section. Complex **9a** shows expected NMR spectroscopic properties and a carbene resonance at δ 181.0 ppm in the $^{13}C\{^1H\}$ NMR spectrum. Complexes **9a** and **9b** show two septets and four doublets for the hydrogen environments of the isopropyl groups in ^{1}H NMR spectra. At room temperature, several resonances are broad and significantly sharpen when

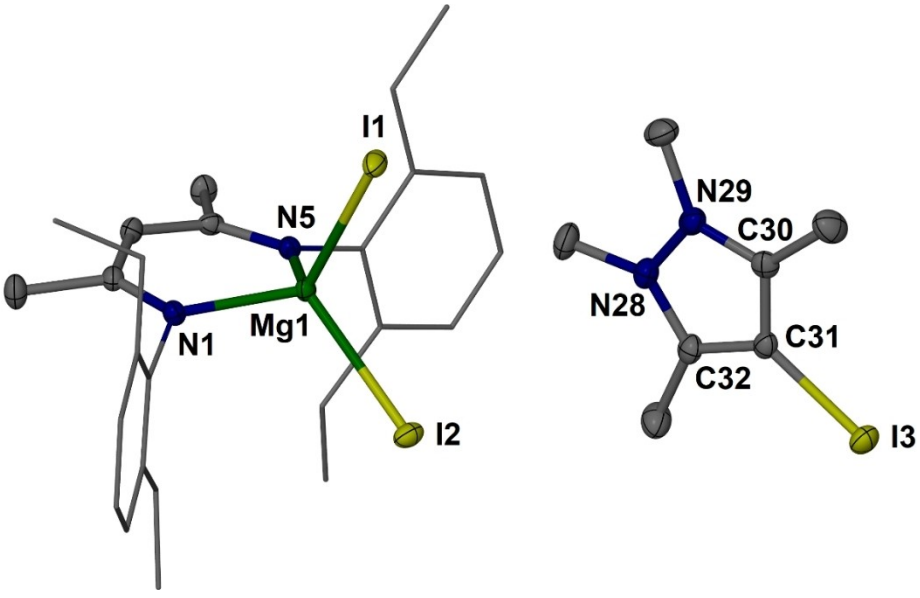

Figure 3. Molecular structure (30 % thermal ellipsoid) of complex **7ab**·2 C_7H_8. Hydrogen atoms, minor components of disorder and solvent molecules omitted for clarity. Dep groups are shown as wireframe. Selected bond lengths (Å) and angles (°): I1–Mg1 2.7363(9), Mg1–I2 2.7279(10), Mg1–N1 2.037(2), Mg1–N5 2.045(2); I2–Mg1–I1 104.08(3), N1–Mg1–N5 93.35(10). Selected distances for the cation are collected in Table 1.

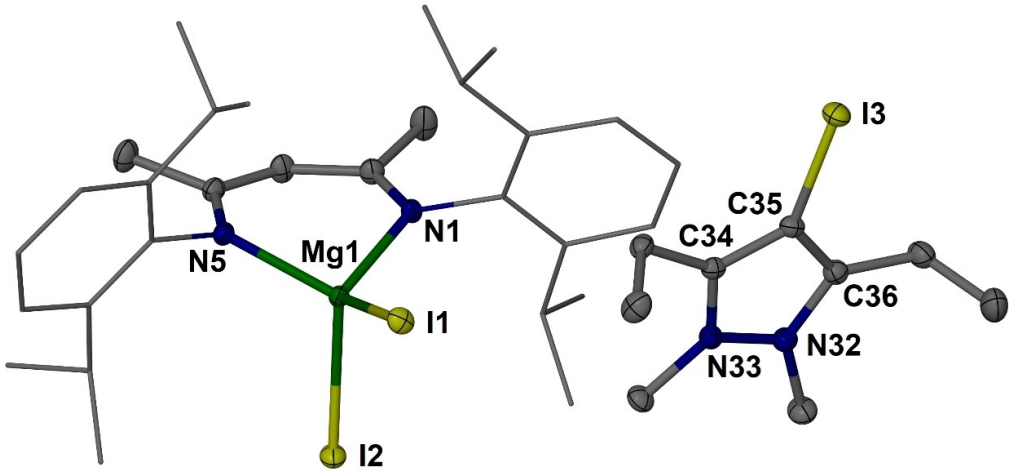

Figure 4. Molecular structure (30% thermal ellipsoid) of complex **7ba**·2 C_7H_8. Hydrogen atoms, and solvent molecules omitted for clarity. Dip groups are shown as wireframe. Selected bond lengths (Å) and angles (°): I1–Mg1 2.7052(6), Mg1–I2 2.7294(6), Mg1–N1 2.0398(15), Mg1–N5 2.0436(16); I1–Mg1–I2 106.69(2), N1–Mg1–N5 95.87(6). Selected distances for the cation are collected in Table 1.

Table 1. Selected distances in iodopyrazolium and iodoimidazolium cations.

Bond type	**7ab**	**7ba**	**8**
C–I/Å	I3–C31 2.070(3)	I3–C35 2.0707(19)	I1–C3 2.092(4)
N–N/Å	N28–N29 1.357(4)	N32–N33 1.365(2)	–
C–N/Å	N28–C32 1.337(4)	N32–C36 1.343(2)	N1–C3 1.336(4)
	N29–C30 1.332(4)	N33–C34 1.337(2)	C3–N1′ 1.336(4)
			N1–C4 1.391(4)
C–C/Å	C30–C31 1.376(4)	C34–C35 1.389(3)	C4–C4′ 1.358(7)
	C31–C32 1.380(4)	C35–C36 1.389(3)	

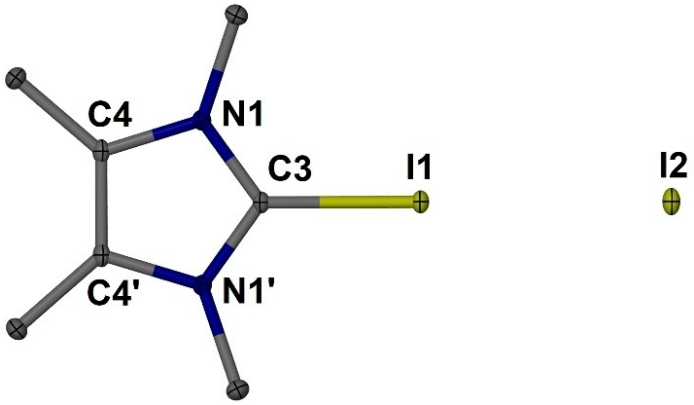

Figure 5. Molecular structure (30% thermal ellipsoid) of complex **8**·$CHCl_3$. Hydrogen atoms and solvent molecule omitted for clarity. I1···I2 3.3337(4) Å. Selected distances for the cation are collected in Table 1.

recorded at 75 °C, more so for the ^{Me}NHC derivative **9a** compared with ^{Et}NHC analogue **9b**.

Computational studies

To gain further insights into the isomeric carbene species and their magnesium complexes, we carried out a DFT study at the M06/def2-TZVP level of theory of a cut-back model of complexes [(^{Dip}nacnac)MgI(^{Me}PZ)] **6a** and [(^{Dip}nacnac)MgI(^{Me}NHC)] **9a** with methyl groups instead of Dip

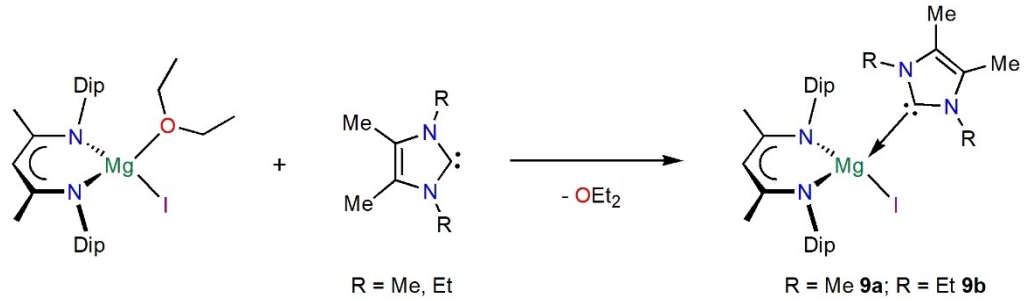

Scheme 3. Synthesis of NHC-complexes **9**.

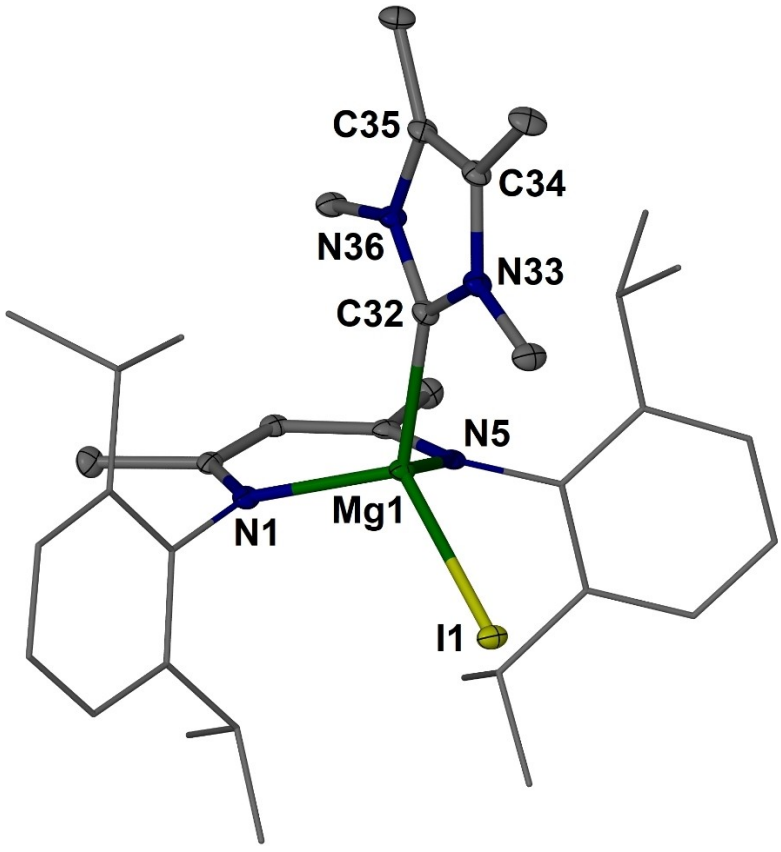

Figure 6. Molecular structure (30 % thermal ellipsoid) of complex **9a**·1.5 C_6H_6. Hydrogen atoms, and solvent molecules omitted for clarity. Dip groups are shown as wireframe. Selected bond angles (°): N1–Mg1–N5 92.39(14), C32–Mg1–I1 113.85(12), N36–C32–N33 102.9(3). Selected distances for the molecule are collected in Figure 8.

substituents, [(^{Me}nacnac)MgI(^{Me}PZ)] **6x** and [(^{Me}nacnac)MgI(^{Me}NHC)] **9x**, and the free isomeric pyrazol-4-ylidene ^{Me}PZ and *N*-heterocyclic carbene ^{Me}NHC. The optimised geometries of the molecules agree well with the available data from X-ray diffraction. Bond distance data of **6a**,**x**, **9a**,**x**, ^{Me}PZ, and ^{Me}NHC is summarised in Figure 8 together with NPA and QTAIM charges and Wiberg bond indices. The range of bond lengths in ^{Me}PZ and for the coordinated fragment in **6a**,**x** are close to those found in related Pd complexes such as **D**.[10] The nitrogen centres in ^{Me}PZ (sum of angles 359.1°) and for the coordinated species in **6x** (359.5° mean) are almost planar, whereas those obtained from the X-ray structure of **6a** are planar within error margins (359.8(8), 360.0(8)). It is worth noting that the related examples **B** and **C** show significantly pyramidalised nitrogen centres, for example with a respective sum of angles of 349° (mean) for **B**.[5] These effects from the nature of the substituents in 3,5-position, and other properties including Wiberg bond indices, are in line with those found in a computational study, including on models of **B** and **C**.[5] π-donor substituents in 3 and 5-position of the ring have also been shown to significantly decrease the aromaticity of the heterocycles.[7]

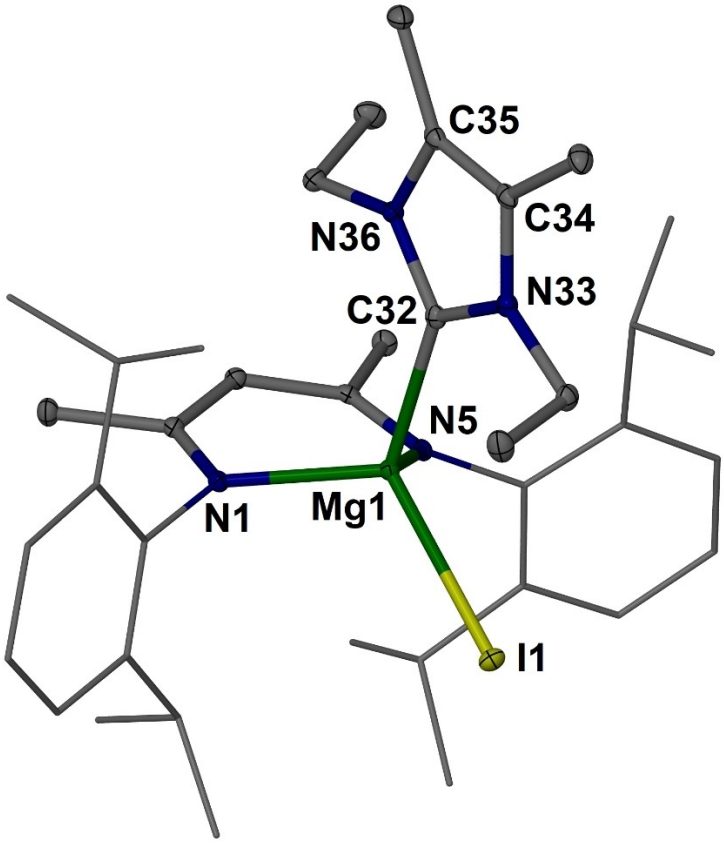

Figure 7. Molecular structure (30% thermal ellipsoid) of complex **9b**. Only one of two independent molecules with highly similar metrical features is shown. Hydrogen atoms, and solvent molecules omitted for clarity. Dip groups are shown as wireframe. Selected bond lengths (Å) and angles (°) for the shown molecule: I1–Mg1 2.6997(6), Mg1–N1 2.0699(16), Mg1–N5 2.0492(16), Mg1–C32 2.2462(19); N5–Mg1–N1 93.15(6); C32–Mg1–I1 114.40(5); N33–C32–N36 103.46(15).

Selected orbitals with energy levels of ^{Me}PZ and ^{Me}NHC are presented in Figure 9 and selected orbitals of **6x** and **9x** are shown in Figure 10. ^{Me}PZ shows a higher HOMO and lower LUMO energy level compared with ^{Me}NHC and, accordingly, a smaller HOMO-LUMO gap (4.91 eV versus 6.59 eV). Inspecting the range of orbitals and Wiberg bond indices (Figure 8) allows us to see why descriptions including cyclic bent allenes and carbenes have been used for ^{Me}PZ and related species,[5–9,30] and highlights differences and similarities to the more common imidazol-2-ylidenes. Both small molecules show a carbene-type lone pair in their HOMOs and this is reflected in Mg–C interactions in **6x** (HOMO-5 and minor in HOMO-9) and **9x** (HOMO-7 and minor in HOMO-9), see Figure 10. Because the pairs ^{Me}PZ, and ^{Me}NHC, and **6x** and **9x**, are isomers we compared their energies. ^{Me}PZ is significantly less stable ($\Delta G = +45.4$ kcal/mol, $\Delta H = +46.1$ kcal/mol) than ^{Me}NHC, although this difference is reduced by around 10 kcal/mol when these nucleophilic molecules are coordinated to the (^{Me}nacnac)MgI fragment ($\Delta G = +36.2$ kcal/mol, $\Delta H = +36.5$ kcal/mol). The ^{Me}-PZ molecule and ligand show a significant negative charge on its carbene carbon atom from both NPA and QTAIM methods, whereas the carbene centre in ^{Me}NHC is approximately charge neutral according to NPA or significantly positively charged based on QTAIM analysis (Figure 8). Independent of the method, the charge of the carbon donor centre in ^{Me}PZ is significantly more negative than that for ^{Me}NHC. Calculated charges for magnesium and iodine atoms agree well between the two methods. The Mg–C bond is slightly shorter in **6x** compared with **9x** for both the DFT and X-ray data. Laplacian maps from QTAIM studies (Figure 11) show a similar overall picture between these molecules, and the bond critical point on the Mg–C bond path shows a slightly higher electron density value for **6x** compared with **9x**. Taken together, all these observations are in line with pyrazol-4-ylidenes acting as significantly better σ-donors in comparison with Arduengo-type *N*-heterocyclic carbenes.[1,2,4]

Conclusion

We have studied the reactions of dimagnesium(I) complexes [{(^{Ar}nacnac)Mg}$_2$] **1** with the iodoarenes iodobenzene and two 4-iodopyrazolium iodide salts. In preliminary reactions with iodobenzene, Grignard-type species [{(^{Ar}nacnac)Mg}$_2$(μ-Ph)(μ-I)], Ar = Dep (**4b**) or Mes (**4c**), were obtained according to NMR spectroscopy, whereas for Ar = Dip, the complexes

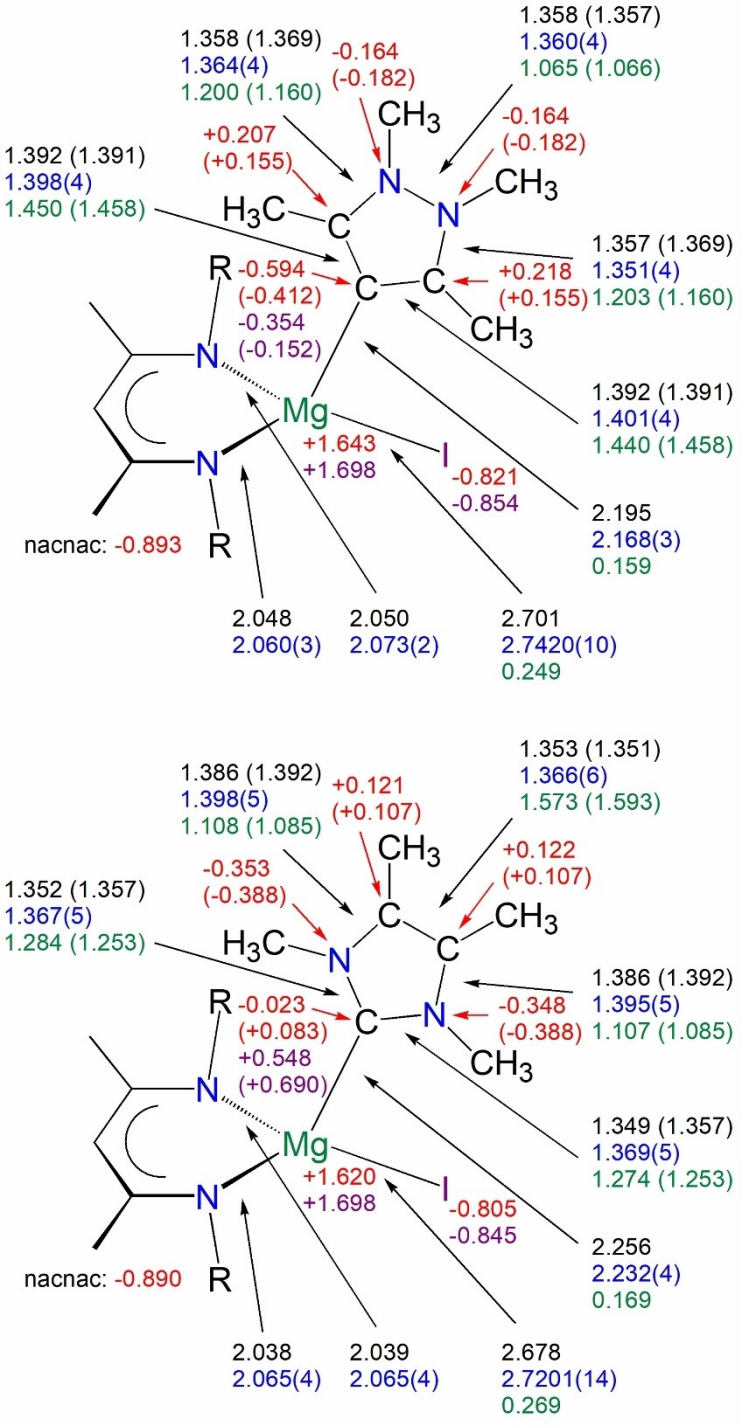

Figure 8. Selected data for complexes **6a**,**x** (top) and **9a**,**x** (bottom); R = Dip (**a**), Me (**x**). Bond distances from DFT studies (black values) and single crystal X-ray diffraction (blue values) are given in Å. Red values show natural population analysis (NBO) charges, purple values report QTAIM charges, and green values provide Wiberg bond indices. Values in parentheses are for the calculated uncoordinated carbene species.

[(^{Dip}nacnac)MgPh] **2a** and [{(^{Dip}nacnac)MgI}$_2$] **3a** were observed for steric reasons. From reactions of **1** with 4-iodopyrazolium iodide salts, we structurally characterised the pyrazol-4-ylidene complex [(^{Dip}nacnac)MgI(^{Me}PZ)] **6a**, but the compound was not isolated in pure form. Salts [^{Me}PZI][(^{Dep}nacnac)MgI$_2$] **7ab** and [^{Et}PZI][(^{Dip}nacnac)MgI$_2$] **7ba** were structurally characterised as other reaction products. Complex **6a** represents the first pyrazol-4-ylidene complex without palladium. The imidazol-2-ylidene complex [(^{Dip}nacnac)MgI(^{Me}NHC)] **9a** was prepared as a constitutional isomer of **6a** and a comparative computational

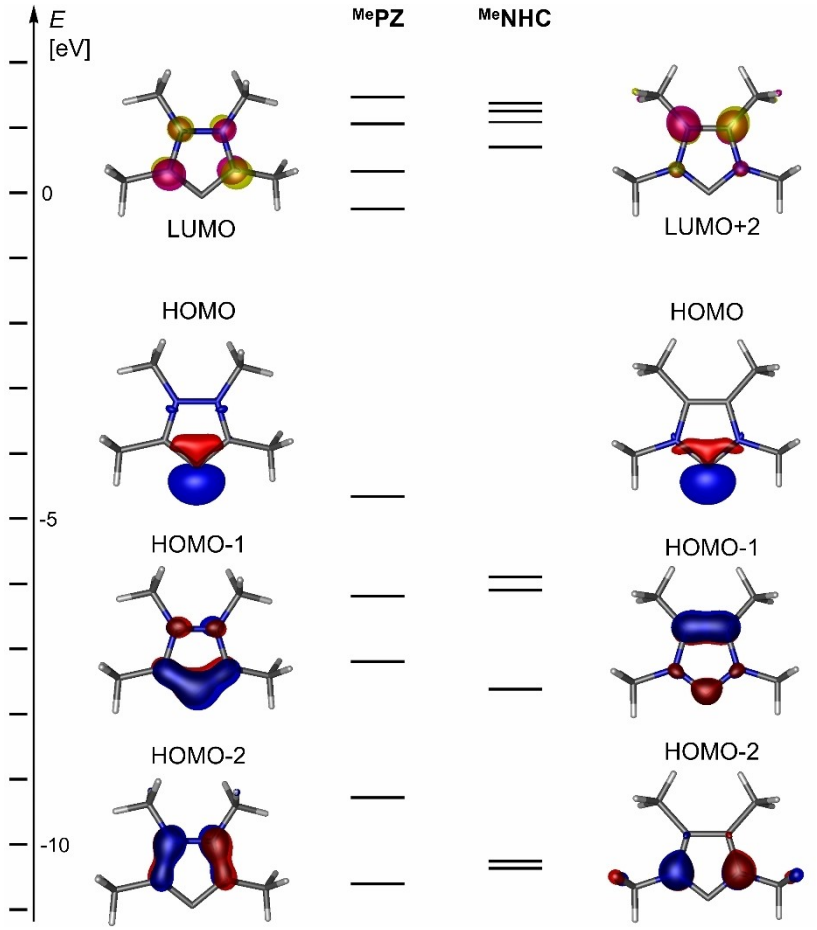

Figure 9. Selected orbitals and energy levels of ^{Me}PZ and ^{Me}NHC (isovalue 0.09).

and structural study between pyrazol-4-ylidene, ^{Me}PZ, and imidazol-2-ylidene, ^{Me}NHC, including their magnesium complexes confirmed the higher thermodynamic energy and more nucleophilic character of ^{Me}PZ over ^{Me}NHC. The pyrazol-4-ylidene ligand shows cyclic bent allene character that provides a nucleophilic carbene donor functionality, and the study highlights the differences and similarities between the two species.

Experimental Section

General considerations. All manipulations, except the syntheses of the iodopyrazoles, were carried out using standard Schlenk and glove box techniques under an atmosphere of high purity argon or dinitrogen. Benzene, toluene, *n*-hexane and THF were either dried and distilled under inert gas over $LiAlH_4$, sodium or potassium, or taken from an MBraun solvent purification system and degassed prior to use. $CDCl_3$ and DMSO-d_6 were used as received for stable organic molecules. ^{1}H and ^{13}C{^{1}H} NMR spectra were recorded on a Bruker AVII 400 or Bruker AV III 500 spectrometer in deuterated benzene and were referenced to the residual ^{1}H or ^{13}C{^{1}H} resonances of the solvent used. Selected NMR spectra are collected in the supporting information. Details on the molecular structures from single crystal X-ray diffraction (Deposition Numbers 2177891–2177897) and computational studies are provided in the supporting information. The syntheses of [{(^{Dip}nacnac)Mg}$_2$],[18] [{(^{Dep}nacnac)Mg}$_2$],[19] [{(^{Mes}nacnac)Mg}$_2$],[20] [(^{Dip}nacnac)MgI(OEt$_2$)],[20] 1,3,4,5-tetramethylimidazol-2-ylidene and 1,3-diethyl-4,5-dimethylimidazol-2-ylidene[31] were performed according to literature procedures. PhI was degassed prior to use and stored over activated molecular sieves under an Ar atmosphere and transferred using a micropipette. All other compounds were used as received from chemical suppliers.

Reactions of [{(^{Ar}nacnac)Mg}$_2$] 1 with PhI to Grignard complexes. Ar = Dip: In a J.Young NMR tube, PhI (2.53 µl, 23 µmol) was added to a solution/slurry of [{(^{Dip}nacnac)Mg}$_2$] **1a** (20 mg, 23 µmol) in C_6D_6 (*ca.* 0.4 ml) and the NMR tube was vigorously shaken. The yellow solution immediately decolourised upon PhI addition and shaking. Full conversion of **1a** to [(^{Dip}nacnac)MgPh] **2a** and [{(^{Dip}nacnac)MgI}$_2$] **3a** was observed by NMR spectroscopy at the first point of analysis after approximately 15 min. Over a period of two hours, **3a** gradually crystallised out of solution at room temperature. NMR spectroscopic data for [(^{Dip}nacnac)MgPh][21] **2a**: ^{1}H NMR (499.9 MHz, C_6D_6): $\delta = 1.16$ (d, $J = 6.9$ Hz, 24H, ArCH(CH_3)$_2$), 1.21 (d, $J = 6.9$ Hz, 24H, ArCH(CH_3)$_2$), 1.71 (s, 12H, NCCH_3), 3.20 (sept, $J = 6.9$ Hz, 8H, ArC*H*(CH$_3$)$_2$), 4.98 (s, 2H, NCC*H*), 6.82 (dd, 5H, $J = 6.2$, 3.0 Hz, 5H, Ar*H*), 7.04 (dd, $J = 4.9$, 1.8 Hz, 10H, Ar*H*), 7.06–7.23 (m, 12H, Ar*H*) ppm. [{(^{Dip}nacnac)MgI}$_2$][22] **3a**: ^{1}H NMR (499.9 MHz, C_6D_6): $\delta = 1.02$ (d, 24H, $J = 6.8$ Hz, 24H, ArCH(CH_3)$_2$), 1.15 (d, 24H, $J = 7.1$ Hz, ArCH(CH_3)$_2$), 1.50 (s, 12H, NCCH_3), 3.19 (sept, 8H, $J = 6.9$ Hz, 8H, ArC*H*(CH$_3$)$_2$), 4.70 (s, 2H, NCC*H*), 7.07 (d, $J = 7.6$ Hz, 10H, Ar*H*) ppm.

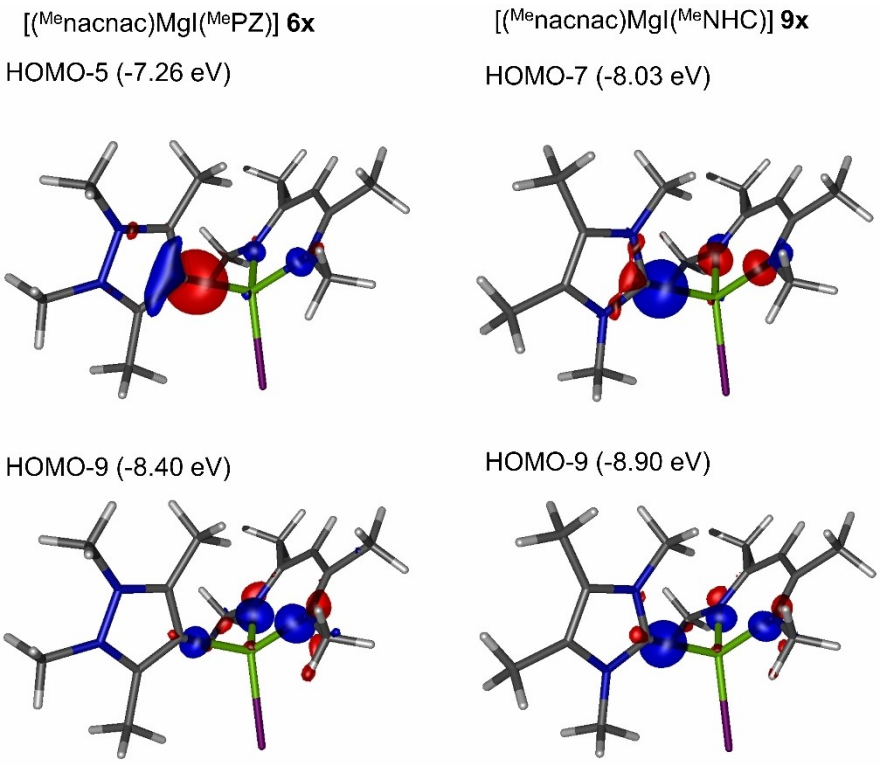

Figure 10. Selected orbitals of [(Menacnac)MgI(MePZ)] **6x** (left) and [(Menacnac)MgI(MeNHC)] **9x** (right) (isovalue 0.09) showing Mg–C contributions.

NB: resonances for **3a** are consistent with those previously described in the literature. **Ar = Dep**: In a J.Young NMR tube, PhI (2.18 µl, 19 µmol) was added to a solution of [{(Depnacnac)Mg}$_2$] **1b** (15 mg, 19 µmol) in C_6D_6 (*ca.* 0.4 ml) and the NMR tube was vigorously shaken. Over 90% conversion was observed at the first point of analysis, however, full conversion of **1b** to [{(Depnacnac)Mg}$_2$(μ-Ph)(μ-I)] **4b** was observed by ^{1}H NMR spectroscopy only after three hours at room temperature. ^{1}H NMR (400.1 MHz, C_6D_6): δ = 0.90 (t, J = 7.5 Hz, 12H, ArCH$_2$C*H*$_3$), 1.31 (t, J = 7.6 Hz, 12H, ArCH$_2$C*H*$_3$), 1.48 (s, 12H, NCC*H*$_3$), 1.70 (dq, J = 15.4, 7.5 Hz, 4H, ArC*H*$_2$CH$_3$), 1.91 (4H, J = 15.1, 7.5 Hz, dq, ArC*H*$_2$CH$_3$), 2.79 (dq, J = 15.3, 7.6 Hz, 4H, ArC*H*$_2$CH$_3$), 2.91 (dq, J = 15.1, 7.5 Hz, 4H, ArC*H*$_2$CH$_3$), 4.76 (s, 2H, NCC*H*), 6.08 (dd, J = 7.6, 1.4 Hz, 3H, MgPh*H*), 6.50 (t, J = 7.5 Hz, 2H, MgPh*H*), 6.95 (m, 1H, MgPh*H*), 7.13–7.18 (m, 14H, Ar*H*), 7.18 (s, 4H, Ar*H*) ppm. ^{13}C{^{1}H} NMR(C_6D_6, 100.6 MHz): δ = 13.3 (ArCH$_2$C*H*$_3$), 14.3 (ArCH$_2$C*H*$_3$), 23.8 (NC*C*H$_3$), 24.7 (ArC*H*$_2$CH$_3$), 25.3 (ArC*H*$_2$CH$_3$), 95.1 (NC*C*H), 125.0 (Ar*C*), 125.2 (Ar*C*), 126.6 (Ar*C*), 129.2 (MgPh*C*), 131.6 (MgPh*C*), 137.1 (Ar*C*), 137.9, (Ar*C*) 145.4 (MgPh*C*), 146.8 (Ar*C*), 151.8 (MgPhC_{ipso}), 168.6 (NCCH$_3$). **Ar = Mes**: In a J.Young NMR tube, PhI (2.35 µL, 21 µmol) was added to a solution/slurry of [{(Mesnacnac)Mg}$_2$] **1c** (15 mg, 21 µmol) in C_6D_6 (*ca.* 0.4 ml) and the NMR tube was vigorously shaken. Full conversion of **1c** to [{(Mesnacnac)Mg}$_2$(μ-Ph)(μ-I)] **4c** was observed by ^{1}H NMR spectroscopy at the first point of analysis after approximately 15 minutes. ^{1}H NMR (499.9 MHz, C_6D_6): δ = 1.48 (br overlaying s, 12H, Ar-*o*-C*H*$_3$; 12H, NCCH$_3$), 2.34 (s, 12H, Ar-*p*-C*H*$_3$), 2.48 (s, 12H, Ar-*o*-C*H*$_3$), 4.80 (s, 2H, NCC*H*), 6.24 (dd, J = 7.4, 1.2 Hz, 2H, MgPh-o-*H*), 6.58 (t, J = 7.5 Hz, 2H, MgPh-m-*H*), 6.68 (s, 6H, Ar*H*), 6.83 (s, 6H, Ar*H*), 7.05 (tt, J = 7.5, 1.4 Hz, 1H, MgPh-*p*-*H*) ppm. ^{13}C{^{1}H} NMR (125.7 MHz, C_6D_6) δ = 18.7 (Ar-*o*-CH$_3$), 20.9 (Ar-*p*-CH$_3$), 21.3 (Ar-*o*-CH$_3$), 23.6 (NCCH$_3$), 95.3 (NCCH), 128.9 (Ar*C*), 129.2 (MgPh-*m*-*C*), 129.9 (Ar*C*), 131.8 (Ar*C*), 132.0 (Ar*C*), 132.6 (Ar*C*), 133.1 (Ar*C*), 145.3 (MgPh-*o*-*C*), 145.4 (Ar*C*), 151.2 (MgPhC_{ipso}), 168.5 (NCCH$_3$) ppm.

Iodopyrazoles and iodopyrazolium salts[9,10,25] were prepared in analogy to previously published methods. **4-Iodo-1,3,5-trimethylpyrazole**. An aqueous solution of "KI$_3$", prepared by dissolving KI (39.7 g, 239 mmol, 3.7 eq.) and I_2 (20.0 g, 78.8 mmol, 1.2 eq.) in H_2O (200 mL), was added dropwise to a solution of 1,3,5-trimethylpyrazole (7.17 g, 65.1 mmol, 1 eq.) and NaOAc (16.0 g, 195.3 mmol, 3 eq.) in H_2O (150 mL). The resulting solution was heated under reflux overnight and cooled to ambient temperature. A saturated aqueous solution of $Na_2S_2O_3$ was added dropwise until the solution turned pale brown. The mixture was neutralised using aqueous $NaHCO_3$ and the crude product was extracted with diethyl ether (6×100 mL). Drying over $MgSO_4$ and removal of the solvent in vacuo afforded the crude product as a pale orange solid that was recrystallized from warm hexane (15 mL, 40 °C). Yield: 6.59 g (43%). ^{1}H NMR (400.1 MHz, $CDCl_3$) δ 2.18 (s, 3H, CC*H*$_3$), 2.23 (s, 3H, CC*H*$_3$), 3.75 (s, 3H, NC*H*$_3$). ^{13}C{^{1}H} NMR (100.6 MHz, $CDCl_3$) δ 12.0 (CCH$_3$), 14.0 (CCH$_3$), 37.0 (NCH$_3$), 62.2 (CI), 140.6 (CCH$_3$), 148.8 (CCH$_3$). **4-Iodo-1,2,3,5-tetramethylpyrazolium iodide 5a**. Iodomethane (5.96 g, 42.0 mmol, 3 eq.) was added to a solution of 4-iodo-1,3,5-trimethylpyrazole (3.31 g, 14.0 mmol, 1 eq.) in THF (20 mL) in a Schlenk flask with J.Young stopcock, and the closed vessel was stirred and heated to 60 °C for four days. The resulting colourless crystalline precipitate was filtered off and dried under vacuum. Yield: 3.54 g (67%). ^{1}H NMR (400.1 MHz, DMSO-d_6) δ 2.46 (s, 6H, CC*H*$_3$), 4.01 (s, 6H, NC*H*$_3$). ^{13}C{^{1}H} NMR (100.6 MHz, DMSO-d_6) δ 13.7 (CCH$_3$), 35.8 (NCH$_3$), 69.6 (CI), 147.6 (CCH$_3$).

3,5-Diethyl-4-iodo-1-methylpyrazole. An aqueous solution of "KI$_3$", prepared by dissolving KI (17.6 g, 106 mmol, 4.2 eq.) and I_2 (8.9 g, 35.1 mmol, 1.4 eq.) in H_2O (100 mL), was added dropwise to a

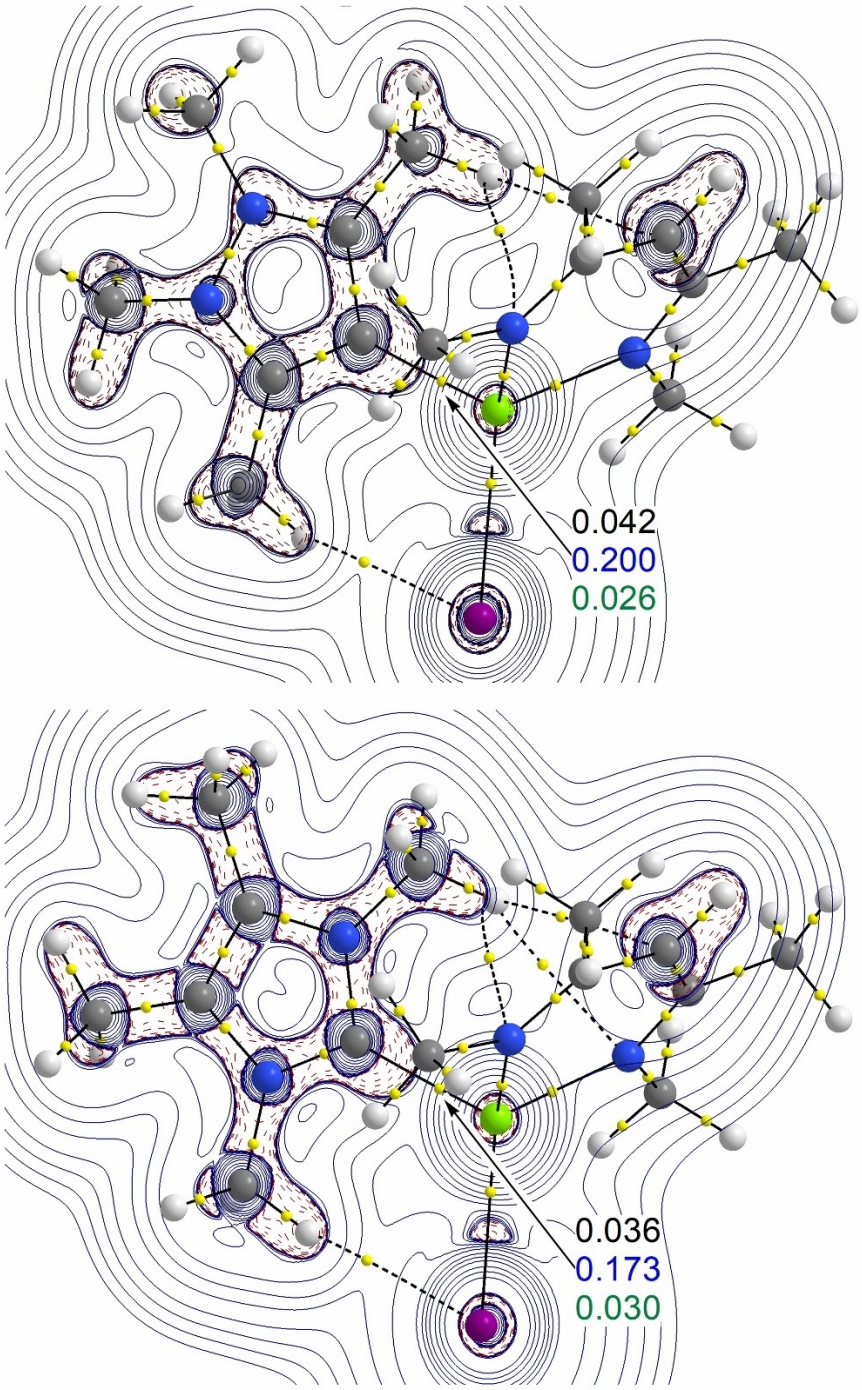

Figure 11. QTAIM contour plots of the Laplacian of the electron density (solid lines positive, dashed lines negative) of [(^{Me}nacnac)MgI(^{Me}PZ)] **6x** (top) and [(^{Me}nacnac)MgI(^{Me}NHC)] **9x** (bottom). Values for the electron density, ρ(r) (black) in e/bohr^3, Laplacian, $\nabla^2\rho$(r) (blue) in e/bohr^5, and bond ellipticity, ε (green), are given for the bond critical point (yellow) on the Mg–C bond path (black).

solution of 3,5-diethyl-1-methylpyrazole (3.20 g, 25.4 mmol, 1 eq.) and NaOAc (6.25 g, 76.2 mmol, 3 eq.) in H_2O (80 mL). The resulting solution was heated under reflux overnight and cooled to ambient temperature. A saturated aqueous solution of $Na_2S_2O_3$ was added dropwise until the solution turned pale brown. The mixture was neutralised using aqueous $NaHCO_3$ and the crude product was extracted with diethyl ether (3×80 mL). Drying over $MgSO_4$ and removal of the solvent in vacuo afforded the crude product as a brown oil that was purified by vacuum distillation (*ca.* 85 °C, 10^{-2} mbar) to afford an orange oil. Yield: 4.55 g (68 %). ^{1}H NMR (400.1 MHz, $CDCl_3$) δ 1.15 (t, J = 7.6 Hz, 3H, CH_2CH_3), 1.23 (t, J = 7.6 Hz, 3H, CH_2CH_3), 2.57 (q, J = 7.6 Hz, 2H, CH_2CH_3), 2.66 (q, J = 7.6 Hz, 2H, CH_2CH_3), 3.82 (s, 3H, NCH_3). ^{13}C{^{1}H} NMR (100.6 MHz, $CDCl_3$) δ 12.9 (CH_2CH_3), 13.4 (CH_2CH_3), 19.6 (CH_2CH_3), 21.8 (CH_2CH_3), 36.9 (NCH_3), 60.0 (*C*I), 145.5 (*C*Et), 153.8 (*C*Et). **3,5-Diethyl-4-iodo-1,2-dimethylpyrazolium iodide 5b**. Iodomethane (9.22 g,

65.0 mmol, 3.8 eq.) was added to a solution of 3,5-diethyl-4-iodo-1-methylpyrazole (4.55 g, 17.2 mmol, 1 eq.) in THF (20 mL) in a Schlenk flask with J.Young stopcock, and the closed vessel was stirred and heated to 60 °C for four days. The resulting colourless crystalline precipitate was filtered off and dried under vacuum. Yield: 6.02 g (86 %). ^{1}H NMR (400.1 MHz, DMSO-d$_6$) δ 1.12 (t, $^3J_{HH=}$ 7.6 Hz, 6H, CH_2CH_3), 2.86 (q, $^3J_{HH=}$ 7.6 Hz, 4H, CH_2CH_3), 4.03 (s, 6H, NCH_3). ^{13}C{^{1}H} NMR (100.6 MHz, DMSO-d$_6$) δ 12.3 (CH_2CH_3), 20.5 (CH_2CH_3), 35.3 (NCH_3), 65.4 (*C*I), 151.5 (*C*Et).

Reactions of [{(^{Ar}nacnac)Mg}$_2$] 1a and 1b with iodopyrazolium iodides. [{(^{Ar}nacnac)Mg}$_2$] **1a** or **1b** (1 eq.) and 4-iodopyrazolium iodide salts **5a** or **5b** (1 eq.) were reacted in a Schlenk flask in toluene, benzene or hexane with vigorous stirring, or in an NMR tube with J.Young top in deuterated benzene, and reacted at room temperature for between 6 h to three days. The suspensions gradually turned colourless, and the mixtures were filtered. In all cases, NMR spectroscopy showed that both the precipitate and the residues in solution contained mixtures of products with approximately 4–5 main β-diketiminate-containing species including large quantities of [{(^{Ar}nacnac)MgI}$_2$] **3a** or **3b**. The complexes [(^{Dip}nacnac)MgI(^{Me}PZ)] **6a**, [^{Me}PZI][(^{Dep}nacnac)MgI$_2$] **7ab** and [^{Et}PZI][(^{Dip}nacnac)MgI$_2$] **7ba** were structurally characterised from these mixtures.

Synthesis of 2-iodo-1,3,4,5-tetramethylimidazolium iodide, [^{Me}NHCI]I, 8. The compound was synthesised as previously reported[32] from the rapid reaction of ^{Me}NHC with I_2 in THF that formed a white crystalline precipitate, and the complex was structurally characterised from crystals grown in chloroform. ^{1}H NMR (400.1 MHz, DMSO-d$_6$): δ 2.29 (s, 6H, CCH_3), 3.72 (s, 6H, NCH_3). ^{13}C{^{1}H} NMR (100.6 MHz, DMSO-d$_6$): δ 9.1 (CCH_3), 36.3 (NCH_3), 104.1 (*C*I), 129.1 (CCH_3). IR (ATR): ν/cm^{-1} 2975w, 2944w, 2915w, 1643 m, 1497 s, 1438 s, 1364 m, 1261 m, 1232 m, 1164 m, 1096 m, 1063 m, 1029 m, 852 s, 800 m, 746 s, 630s.

[(^{Dip}nacnac)MgI(^{Me}NHC)] 9a. A solution of 1,3,4,5-tetramethylimidazol-2-ylidene (0.13 g, 1.05 mmol) in toluene (10 ml) was added to a slurry of [(^{Dip}nacnac)MgI(OEt$_2$)] (0.589 g, 0.916 mmol) in toluene (20 ml) at ambient temperature. The mixture briefly became soluble before turning cloudy again. The reaction mixture was stirred for 30 min and concentrated to *ca.* 10 ml under reduced pressure. Hexane (20 ml) was added, the mixture briefly stirred, and the formed white crystalline precipitate of **9a** was settled, filtered off and dried under vacuum. Crystals suitable for X-ray crystallographic analysis were grown from a concentrated solution in benzene (or hexane). Yield: 0.48 g (76 %); ^{1}H NMR (499.9 MHz, C$_6$D$_6$, 348 K) δ = 0.69 (d, J = 6.9 Hz, 6H, Ar-*o*-CH(CH_3)$_2$), 1.12 (d, J = 6.9 Hz, 6H, Ar-*o*-CH(CH_3)$_2$), 1.33 (d, J = 6.9 Hz, 6H, Ar-*o*-CH(CH_3)$_2$), 1.38 (s, 6H, NCCH_3 (NHC)), 1.66 (d, J = 6.9 Hz, 6H, Ar-*o*-CH(CH_3)$_2$), 1.74 (s, 6H, NCCH_3), 3.06 (sept, J = 6.9 Hz, 2H, Ar-*o*-C*H*(CH_3)$_2$), 3.31 (s, 6H, NCH_3 (NHC)), 3.85 (sept, J = 6.9 Hz, 2H, Ar-*o*-C*H*(CH_3)$_2$), 5.00 (s, 1H, NCC*H*), 7.04 (d, J = 7.4 Hz, 2H, Ar-*m*-*H*), 7.13 (t, J = 7.7 Hz, 2H, Ar-ρ-*H*), 7.26 (d, J = 7.4 Hz, 2H, Ar-*m*-*H*). ^{13}C{^{1}H} NMR (126 MHz, C$_6$D$_6$, 348 K) δ = 8.0 (NCCH_3 (NHC)), 24.1 (NCCH_3), 24.5 (Ar-*o*-CH(CH_3)), 24.6 (Ar-*o*-CH(CH_3)), 24.8 (Ar-*o*-CH(CH_3)), 26.0 (NCH_3 (NHC)), 28.2 (Ar-*o*-C*H*(CH_3)), 28.9 (Ar-*o*-C*H*(CH_3)), 35.4 (NCCH_3 (NHC)), 95.3 (NC*C*H), 123.2 (Ar*C*), 124.9 (Ar*C*), 125.5 (Ar*C*), 142.2 (Ar*C*), 144.3 (Ar*C*), 146.1 (Ar*C*), 168.7 (NCCH_3), 181.0 (N*C*N). IR (ATR): ν/cm^{-1} 3053w, 2957 m, 2923 m, 2866 m, 1540 m, 1512 m, 1457 s, 1433 s, 1398 s, 1381 s, 1365 s, 1313 s, 1259 s, 1228 m, 1171 s, 1099 m, 1014 m, 929 m, 844 m, 790s, 757 s, 731 m, 633 m, 611 m.

[(^{Dip}nacnac)MgI(^{Et}NHC)] 9b. Toluene (50 ml) was added to a mixture of [(^{Dip}nacnac)MgI(OEt$_2$)] (200 mg, 0.311 mmol) and 1,3-diethyl-4,5-dimethylimidazol-2-ylidene **7b** (38.6 mg, 0.311 mmol) at ambient temperature and the resulting colourless solution was stirred for 16 hours. Storing the reaction mixture at −40 °C for one day afforded **9b** as a white powder, which was filtered and dried under vacuum. Concentration and subsequent cooling of the supernatant solution afforded a second crop of **9b**. Crystals suitable for X-ray crystallographic analysis were grown from a concentrated benzene solution. Yield: 138 mg (62 %); ^{1}H NMR (499.9 MHz, benzene-d_6, 348 K) δ = 0.75 (d, J = 6.9 Hz, 6H, Ar-*o*-CH(CH_3)$_2$), 1.02 (br, 6H, NCH_2CH_3 (NHC)), 1.12 (d, J = 6.9 Hz, 6H, Ar-*o*-CH(CH_3)$_2$), 1.32 (d, J = 6.9 Hz, 6H, Ar-*o*-CH(CH_3)$_2$), 1.53 (br, 6H, NC(CH_3) (NHC)), 1.66 (d, J = 6.9 Hz, 6H, Ar-*o*-CH(CH_3)$_2$), 1.73 (s, 6H, NCCH_3), 3.08 (br sept, 2H, Ar-*o*-C*H*(CH_3)$_2$), 3.80 (br sept, 2H, Ar-*o*-C*H*(CH_3)$_2$), 4.04 (br, 4H, NCH_2CH$_3$ (NHC)), 4.95 (s, 1H, NCC*H*), 7.06 (d, J = 7.5 Hz, 2H, Ar-*m*-*H*), 7.13 (t, J = 7.6 Hz, 2H, Ar-ρ-*H*), 7.26 (d, J = 7.6 Hz, 2H, Ar-*m*-*H*). ^{13}C{^{1}H} NMR (126 MHz, C$_6$D$_6$, 348 K) δ = 8.4 (NCCH_3 (NHC)), 16.5 (NCH_2CH_3 (NHC)), 24.5 (NCCH_3), 24.7 (Ar-*o*-CH(CH_3)), 24.9 (Ar-*o*-CH(CH_3)), 25.9 (NCH_2CH_3 (NHC)), 28.0 (Ar-*o*-CH(CH_3)), 28.9 (Ar-*o*-C*H*(CH_3)), 43.7 (NCCH_3 (NHC)), 95.0 (NC*C*H), 123.2 (Ar*C*), 124.9 (Ar*C*), 125.5 (Ar*C*), 142.2 (Ar*C*), 144.3 (Ar*C*), 146.1 (Ar*C*), 168.8 (NCCH_3), 179.9 (N*C*N).

Acknowledgements

We thank the University of St Andrews, the EPSRC doctoral training grant (EP/N509759/1), and the Centre for Doctoral Training in Critical Resource Catalysis (CRITICAT, EP/ L016419/1) for support. Part of this research was undertaken on the MX1 beamline at the Australian Synchrotron, Victoria, Australia. We gratefully acknowledge computational support via the EaStCHEM Research Computing Facility.

Conflict of Interest

The authors declare no conflict of interest.

Data Availability Statement

X-ray crystallography data has been deposited with the CCDC. Further data that support the findings of this study are available in the supplementary material of this article. The research data (NMR and DFT) supporting this publication can be accessed at https://doi.org/10.17630/f77acad3-1e69-4001-b52d-fba8e09f4392.

Keywords: Bent allenes · Carbenes · Grignard reagents · Low oxidation states · Magnesium

[1] a) P. Bellotti, M. Koy, M. N. Hopkinson, F. Glorius, *Nat. Chem. Rev.* **2021**, *5*, 711–725.
[2] a) S. C. Sau, P. K. Hota, S. K. Mandal, M. Soleilhavoup, G. Bertrand, *Chem. Soc. Rev.* **2020**, *49*, 1233–1252; b) D. Munz, *Organometallics* **2018**, *37*, 275–289; c) R. H. Crabtree, *Coord. Chem. Rev.* **2013**, *257*, 755–766; d) M. Melaimi, M. Soleilhavoup, G. Bertrand, *Angew. Chem. Int. Ed.* **2010**, *49*, 8810–8849; *Angew. Chem.* **2010**, *122*, 8992–9032; e) O. Schuster, L. Yang, H. G. Raubenheimer, M. Albrecht, *Chem. Rev.* **2009**, *109*, 3445–3478.
[3] V. Nesterov, D. Reiter, P. Bag, P. Frisch, R. Holzner, A. Porzelt, S. Inoue, *Chem. Rev.* **2018**, *118*, 9678–9842.

[4] a) H. V. Huynh, *Chem. Rev.* **2018**, *118*, 9457–9492; b) D. G. Gusev, *Organometallics* **2009**, *28*, 6458–6461.
[5] V. Lavallo, C. A. Dyker, B. Donnadieu, G. Bertrand, *Angew. Chem. Int. Ed.* **2008**, *47*, 5411–5414; *Angew. Chem.* **2008**, *120*, 5491–5494.
[6] For related species see: a) M. Melaimi, P. Parameswaran, B. Donnadieu, G. Frenking, G. Bertrand, *Angew. Chem. Int. Ed.* **2009**, *48*, 4792–4795; *Angew. Chem.* **2009**, *121*, 4886–4889; b) C. A. Dyker, V. Lavallo, B. Donnadieu, G. Bertrand, *Angew. Chem. Int. Ed.* **2008**, *47*, 3206–3209; *Angew. Chem.* **2008**, *120*, 3250–3253.
[7] I. Fernandez, C. A. Dyker, A. DeHope, B. Donnadieu, G. Frenking, G. Bertrand, *J. Am. Chem. Soc.* **2009**, *131*, 11875–11881.
[8] a) E. Kleinpeter, A. Koch, *Tetrahedron* **2019**, *75*, 1548–1554; Carbodicarbene version: b) G. Frenking, R. Tonner, *Contemporary Carbene Chemistry*, chapter 8, First Edition. Ed. R. A. Moss, M. P. Doyle. John Wiley & Sons, Inc, 2014, pp. 216–236; c) M. M. Hänninen, A. Peuronen, H. M. Tuononen, *Chem. Eur. J.* **2009**, *15*, 7287–7291; d) V. Lavallo, C. A. Dyker, B. Donnadieu, G. Bertrand, *Angew. Chem. Int. Ed.* **2009**, *48*, 1540–1542; *Angew. Chem.* **2009**, *121*, 1568–1570; e) M. Christl, B. Engels, *Angew. Chem. Int. Ed.* **2009**, *48*, 1538–1539; *Angew. Chem.* **2009**, *121*, 1566–1567.
[9] Y. Han, H. V. Huynh, *Dalton Trans.* **2011**, *40*, 2141–2147.
[10] a) Y. Han, L. J. Lee, H. V. Huynh, *Chem. Eur. J.* **2010**, *16*, 771–773; b) Y. Han, L. J. Lee, H. V. Huynh, *Organometallics* **2009**, *28*, 2778–2786; c) Y. Han, H. V. Huynh, G. K. Tan, *Organometallics* **2007**, *26*, 6581–6585; d) Y. Han, H. V. Huynh, *Chem. Commun.* **2007**, 1089–1091; For a related isoxazole derivative see: e) M. Iglesias, M. Albrecht, *Dalton Trans.* **2010**, *39*, 5213–5215.
[11] a) B. Rösch, S. Harder, *Chem. Commun.* **2021**, *57*, 9354–9365; b) C. Jones, *Nat. Chem. Rev.* **2017**, *1*, 0059; c) A. Stasch, C. Jones, *Dalton Trans.* **2011**, *40*, 5659–5672.
[12] a) D. Dange, A. R. Gair, D. D. L. Jones, M. Juckel, S. Aldridge, C. Jones, *Chem. Sci.* **2019**, *10*, 3208–3216; b) A. J. Boutland, A. Carroll, C. A. Lamsfus, A. Stasch, L. Maron, C. Jones, *J. Am. Chem. Soc.* **2017**, *139*, 18190–18193.
[13] a) S. R. Lawrence, D. B. Cordes, A. M. Z. Slawin, A. Stasch, *Dalton Trans.* **2019**, ***48***, 16936–16942; b) S. R. Lawrence, C. A. Ohlin, D. B. Cordes, A. M. Z. Slawin, A. Stasch, *Chem. Sci.* **2019**, *10*, 10755–10764.
[14] a) G. Coates, B. J. Ward, C. Bakewell, A. J. P. White, M. R. Crimmin, *Chem. Eur. J.* **2018**, *24*, 16282–16286; b) C. Bakewell, B. J. Ward, A. J. P. White, M. R. Crimmin, *Chem. Sci.* **2018**, *9*, 2348–2356; c) C. Bakewell, A. J. P. White, M. R. Crimmin, *J. Am. Chem. Soc.* **2016**, *138*, 12763–12766.
[15] B. Rösch, T. X. Gentner, J. Eyselein, J. Langer, H. Elsen, S. Harder, *Nature* **2021**, *592*, 717–721.
[16] A. Stasch, *Chem. Eur. J.* **2012**, *18*, 15105–15112.
[17] J. F. Garst, M. P. Soriaga, *Coord. Chem. Rev.* **2004**, *248*, 623–652.
[18] S. P. Green, C. Jones, A. Stasch, *Science* **2007**, *318*, 1754–1757.
[19] R. Lalrempuia, C. E. Kefalidis, S. J. Bonyhady, B. Schwarze, L. Maron, A. Stasch, C. Jones, *J. Am. Chem. Soc.* **2015**, *137*, 8944–8947.
[20] S. J. Bonyhady, C. Jones, S. Nembenna, A. Stasch, A. J. Edwards, G. J. McIntyre, *Chem. Eur. J.* **2010**, *16*, 938–955.
[21] a) A. P. Dove, V. C. Gibson, P. Hormnirun, E. L. Marshall, J. A. Segal, A. J. P. White, D. J. Williams, *Dalton Trans.* **2003**, 3088–3097; b) for related complexes see: D. D. L. Jones, I. Douair, L. Maron, C. Jones, *Angew. Chem. Int. Ed.* **2021**, *60*, 7087–7092.
[22] C. S. MacNeil, K. R. D. Johnson, P. G. Hayes, R. T. Boeré, *Acta Crystallogr.* **2016**, *E72*, 1754–1756.
[23] M. Garçon, A. J. P. White, M. R. Crimmin, *Chem. Commun.* **2018**, *54*, 12326–12328.
[24] K. G. Pearce, C. Dinoi, M. S. Hill, M. F. Mahon, L. Maron, R. S. Schwamm, A. S. S. Wilson, *Angew. Chem. Int. Ed.* **2022**, *61*, e202200305.
[25] A. A. Sysoeva, A. S. Novikov, M. V. Il'in, V. V. Suslonov, D. S. Bolotin, *Org. Biomol. Chem.* **2021**, *19*, 7611–7620.
[26] a) A. D. Obi, L. A. Freeman, D. A. Dickie, R. J. Gilliard Jr., *Organometallics* **2020**, *39*, 4575–4583; b) A. Stasch, *Angew. Chem. Int. Ed.* **2014**, *53*, 10200–100203; *Angew. Chem.* **2014**, *126*, 10364–10367.
[27] a) D. W. N. Wilson, S. J. Urwin, E. S. Yang, J. M. Goicoechea, *J. Am. Chem. Soc.* **2021**, *143*, 10367–10373; b) A.-F. Pecharman, M. S. Hill, C. L. McMullin, M. F. Mahon, *Angew. Chem. Int. Ed.* **2020**, *59*, 13628–13632; *Angew. Chem.* **2020**, *132*, 13730–13734.
[28] a) K. Yuvaraj, A. Carpentier, C. D. Smith, L. Maron, C. Jones, *Inorg. Chem.* **2021**, *60*, 6065–6072; b) K. Yuvaraj, I. Douair, L. Maron, C. Jones, *Chem. Eur. J.* **2020**, *26*, 14665–14670; c) K. Yuvaraj, I. Douair, A. Paparo, L. Maron, C. Jones, *J. Am. Chem. Soc.* **2019**, *141*, 8764–8768.
[29] D. Jędrzkiewicz, J. Mai, J. Langer, Z. Mathe, N. Patel, S. DeBeer, S. Harder, *Angew. Chem. Int. Ed.* **2022**, *61*, e202200511.
[30] For other computational studies related to pyrazol-4-ylidene see: a) B. Borthakur, B. Silvi, R. D. Dewhurst, A. K. Phukan, *J. Comb. Chem.* **2016**, *37*, 1484–1490; b) B. Borthakur, T. Rahman, A. K. Phukan, *J. Org. Chem.* **2014**, *79*, 10801–10810.
[31] N. Kuhn, T. Kratz, *Synthesis* **1993**, *1993*, 561–562.
[32] D. S. McGuinness, K. J. Cavell, B. F. Yates, B. W. Skelton, A. H. White, *J. Am. Chem. Soc.* **2001**, *123*, 8317–8328.

Manuscript received: June 16, 2022
Revised manuscript received: July 4, 2022
Accepted manuscript online: July 25, 2022

RESEARCH ARTICLE

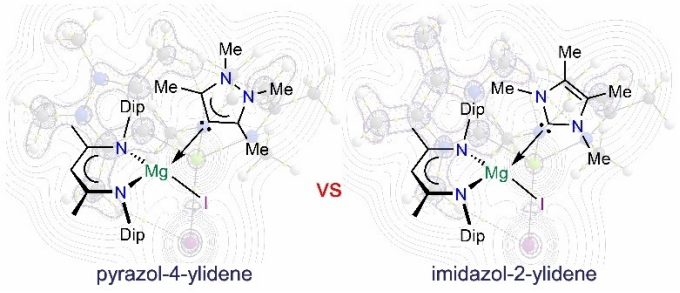

*S. Burnett, M. de Vere-Tucker, M. Davitt, Dr. D. B. Cordes, Prof. Dr. A. M. Z. Slawin, R. Ferns, Dr. T. van Mourik, Dr. A. Stasch**